

Supplementary Materials for
Aire drives steroid hormone biosynthesis by medullary thymic epithelial cells

Matthew D. Taves *et al.*

Corresponding author: Jonathan D. Ashwell, jda@pop.nci.nih.gov; Matthew D. Taves, matthew.taves@cornell.edu

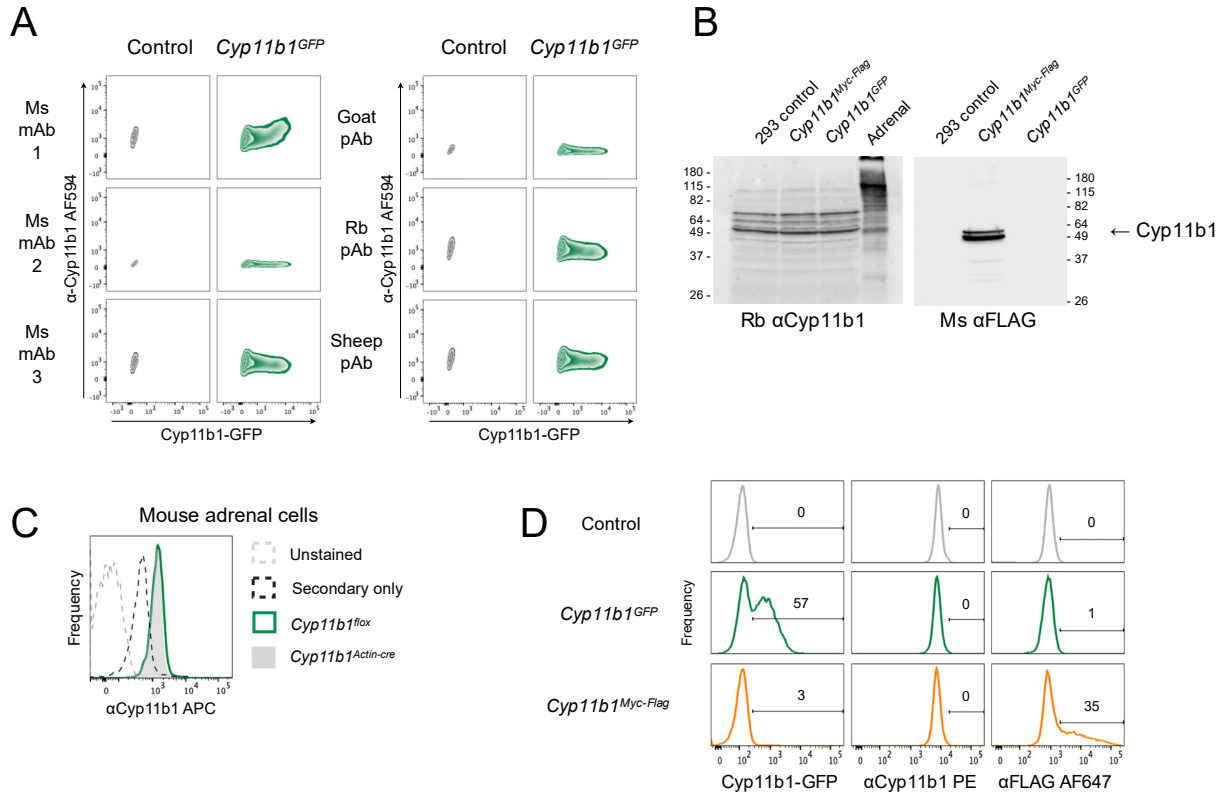
Sci. Immunol. **8**, eabo7975 (2023)
DOI: 10.1126/sciimmunol.abo7975

The PDF file includes:

Figs. S1 to S7
Table S1

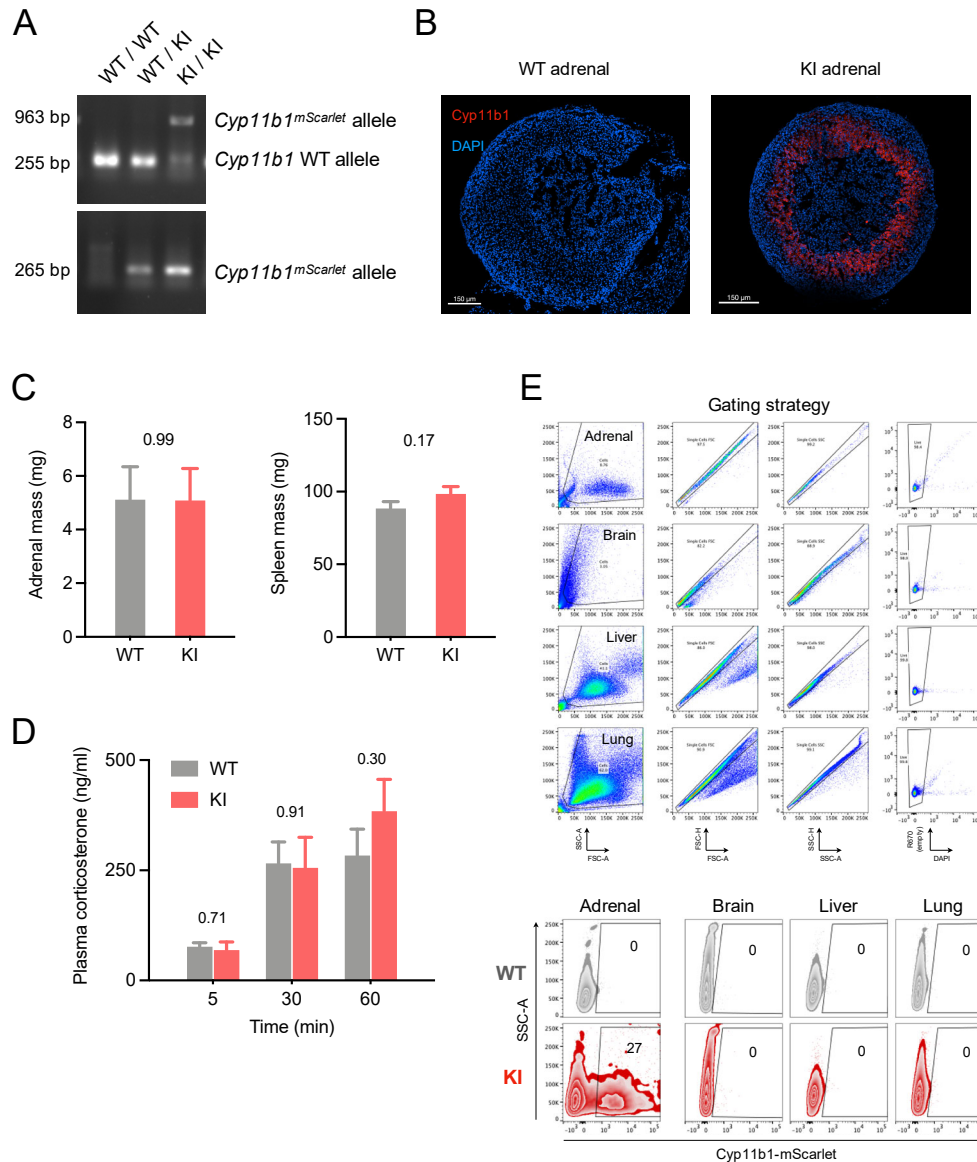
Other Supplementary Material for this manuscript includes the following:

Data files S1 and S2
MDAR Reproducibility Checklist



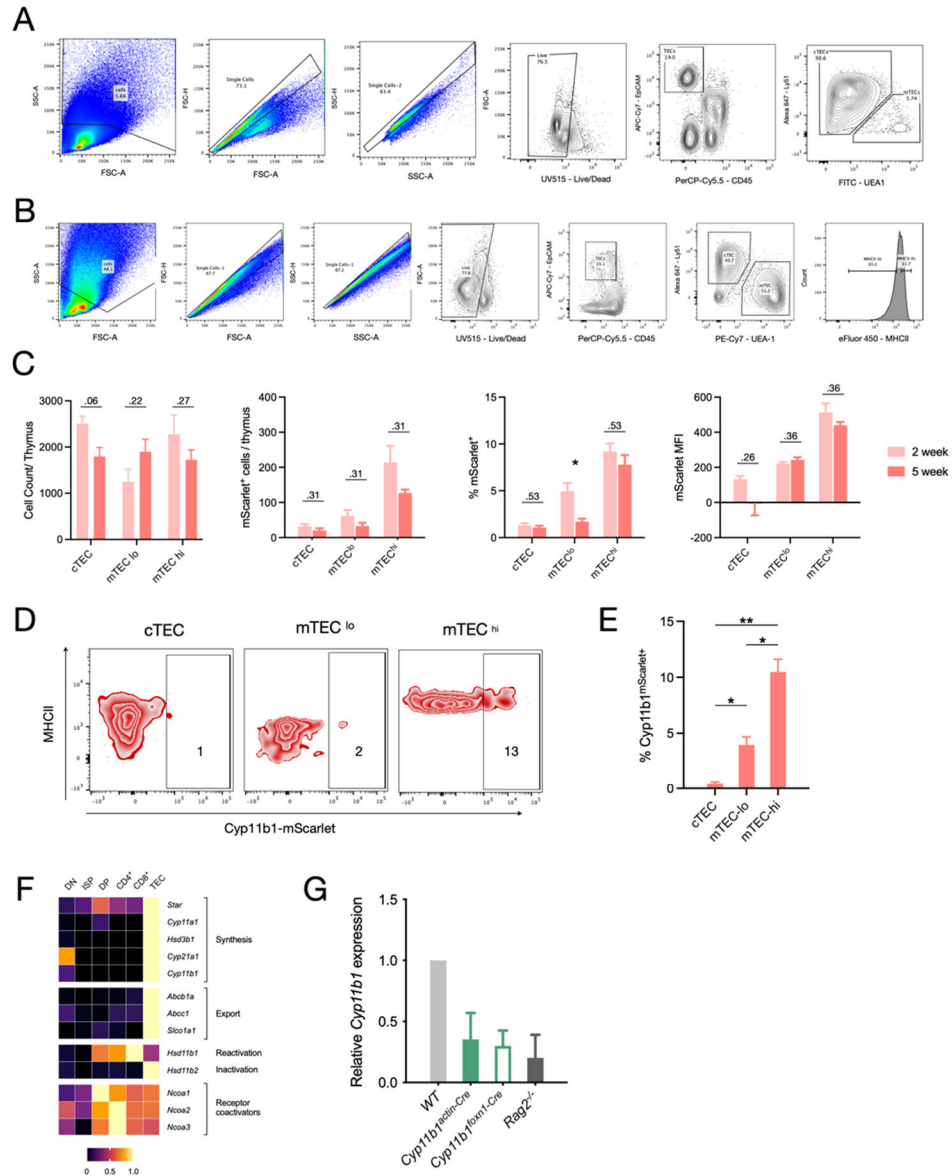
Supplementary Figure 1. *Cyp11b1* is not specifically detected by antibody staining.

(A) HEK 293 cells were transfected with a control vector (grey) or vector encoding a GFP-tagged Cyp11b1 fusion protein (*Cyp11b1^{GFP}*; green), collected 72 h later, fixed, permeabilized, stained with anti-Cyp11b1 primary antibody and Alexa fluor 594-conjugated secondary (αCyp11b1), and data acquired by flow cytometry. Contour plots at left show cells stained with mouse monoclonal antibodies (clones A-11, B-11, H-11) and at right show control and *Cyp11b1^{GFP}* cells stained with goat, rabbit, or sheep polyclonal antibodies. Antibodies were tested in at least two experiments. (B) HEK 293 cells were transfected and harvested as in A) and adrenal cells were collected from WT mice. Cells were boiled in SDS sample buffer, separated by SDS-PAGE, blots stained with anti-Cyp11b1 or anti-FLAG antibody, and detected using HRP-conjugated secondary antibodies with enhanced chemiluminescence substrate. (C) Adrenals from control *Cyp11b1^{fllox/fllox}* or *Cyp11b1*-deficient (*Cyp11b1^{Actin-cre}*) mice were minced, dissociated, fixed, permeabilized, and stained with anti-Cyp11b1 monoclonal antibody (A-11) and APC-conjugated secondary antibody, and data acquired by flow cytometry. (D) HEK 293 cells were transfected with a control vector (grey), *Cyp11b1^{GFP}* vector (green), or vector encoding a Myc-FLAG-tagged Cyp11b1 fusion protein (*Cyp11b1^{Myc-FLAG}*; orange), collected 72 h later, fixed, permeabilized, stained with anti-Cyp11b1 (middle) and anti-FLAG (right) primary antibodies, and PE- and Alexa fluor 647-conjugated secondary antibodies, and data acquired by flow cytometry. Numbers show the percent of cells falling within the positive staining gate. Experiments in A and D were performed once, in B and C were performed twice.



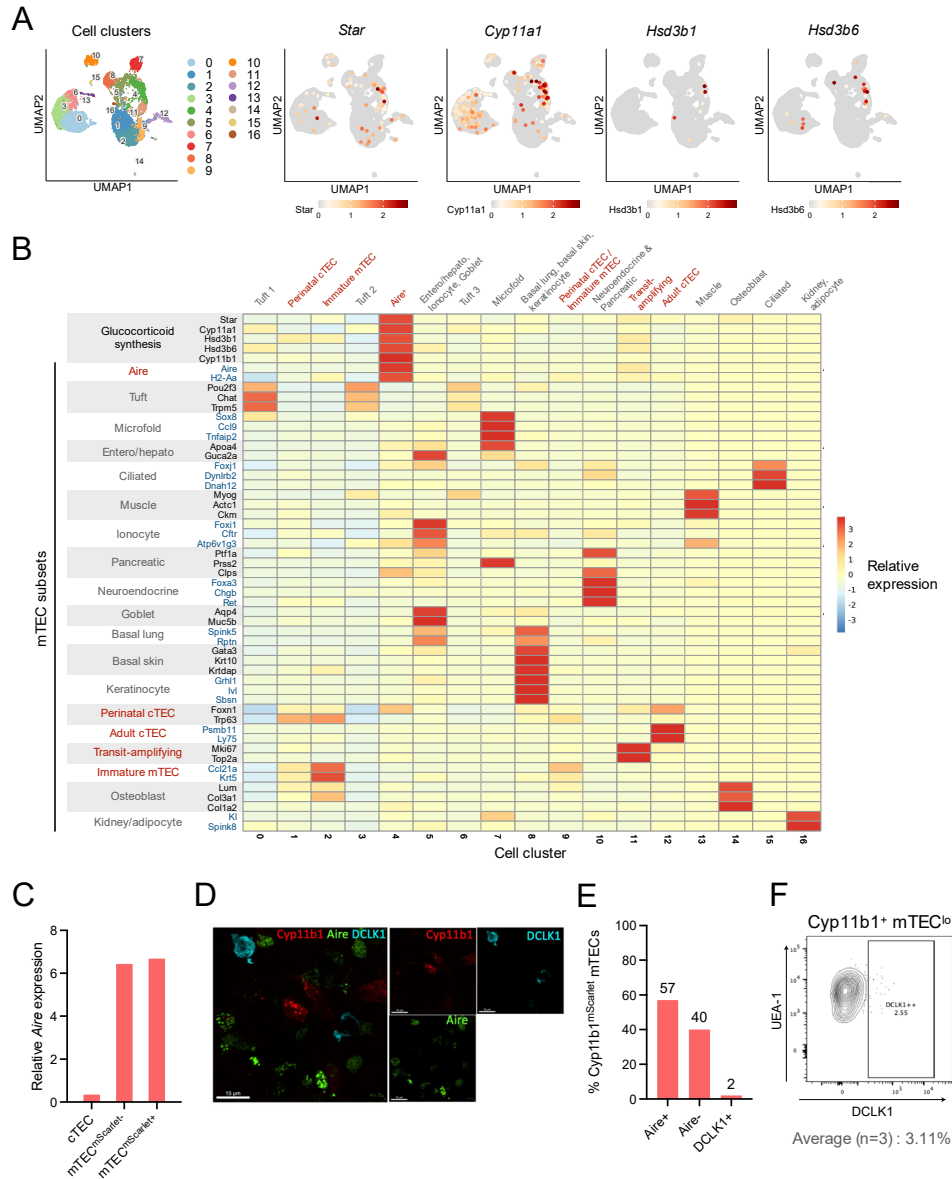
Supplementary Figure 2. *Cyp11b1^{mScarlet}* knock-in reporter mice are phenotypically normal and allow detection of glucocorticoid-synthetic cells

(A) Genomic DNA was extracted from wild-type (WT) and *Cyp11b1^{mScarlet}* knock-in (KI) heterozygous and homozygous mice and assayed using a forward primers upstream and reverse primer downstream of the *mScarlet* sequence (top) or a forward primer upstream and reverse primer within the *mScarlet* sequence (bottom). Amplicons were separated on a 2% agarose gel and visualized with SafeGreen gel stain. (B) WT and KI mouse adrenals were fixed, stained with DAPI, and confocal images taken at 20× magnification. Scale bar = 150 μ m. (C) Adrenals and spleens from WT and KI mice were collected and weighed. Data presented as mean \pm SEM, N = 7 mice per genotype. Numbers above bars give p-value results of unpaired t-tests comparing genotypes. (D) WT and KI mice were anesthetized with isoflurane and blood samples collected at 5 min, 30 min, and 60 min after initial disturbance in the home cage. Data presented as mean \pm SEM, N = 7 mice per genotype. Data were first analyzed with a mixed linear model, giving a significant effect of time ($p < 0.0001$) but no effect of genotype ($p = 0.69$). Numbers above bars give p-value results of follow-up Sidak pairwise comparison tests between genotypes at each time. (E) Tissues from WT and KI mice were dissected, digested in trypsin-EDTA, stained with DAPI and data acquired by flow cytometry. Contour plots show live single cells, and numbers indicate the percent of cells within the mScarlet⁺ gate. Data are representative of two independent experiments.



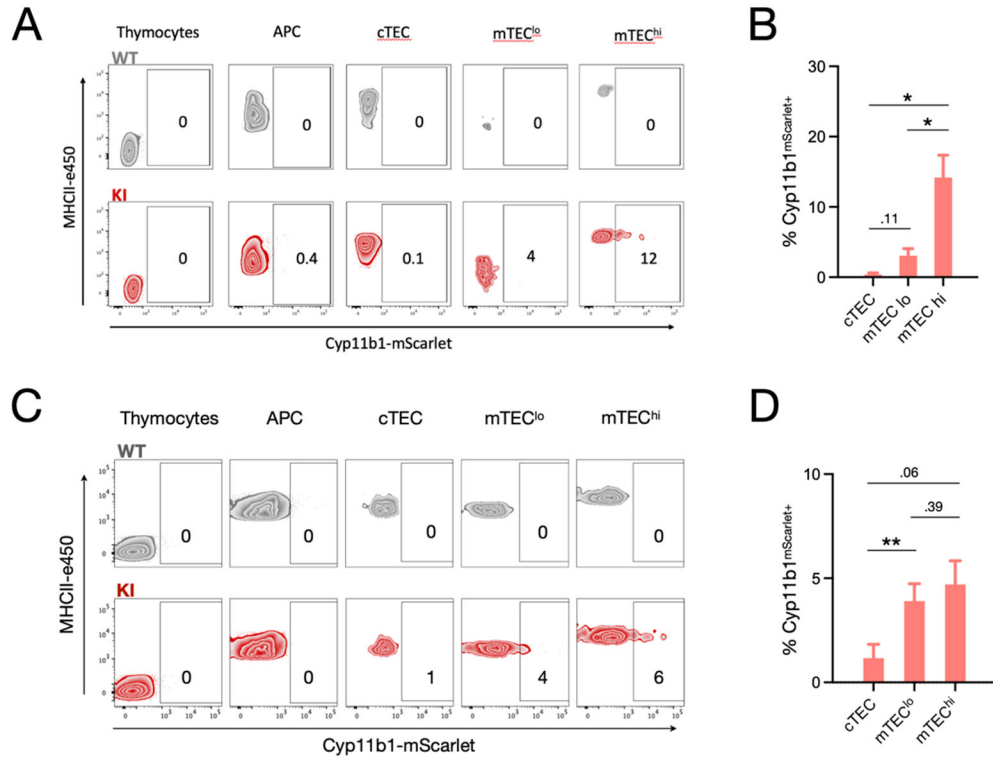
Supplementary Figure 3. De novo glucocorticoid synthesis in the thymus by mTEC.

(A-B) Gating strategy for flow cytometry analysis of thymic epithelial cells (TEC). Shown are representative thymi from mice at (A) embryonic day 18.5 (E18.5) and at (B) postnatal week 2. (C) Numbers and proportions of mScarlet⁺ TEC in 2-week and 5-week old thymi. Data are presented as mean ± SEM with n = 7 two-week and 6 five-week mice, and analyzed with an unpaired t-test with significance shown as * p < 0.05 and ** p < 0.01, after applying the Holm correction to control family-wise error at 0.05. (D) Thymi from embryonic day 18.5 mice were digested and cells analyzed by flow cytometry. Contour plots show each subset and numbers indicate the percent of cells within the mScarlet⁺ gate. (E) Data collected and analyzed as in panel C, pooled from two experiments with embryonic day 18.5 mice, with results of pairwise comparisons indicated as * p < 0.05 and ** p < 0.01. (F) Gene expression of glucocorticoid biosynthetic enzymes, transporters, metabolite reactivation/inactivation enzymes, and receptor coactivator genes in thymocyte and TEC subsets of the thymus. Bulk RNA-seq data were acquired from the ImmGen database, and each gene is shown relative to its maximum expression level across analyzed cell types. (G) Whole thymi were collected from wild-type (WT), Cyp11b1-deficient (*Cyp11b1^{actin-Cre}*), Cyp11b1 conditional knockout (*Cyp11b1^{foxn1-Cre}*), and *Rag2*-deficient mice, total RNA extracted, and *Cyp11b1* gene expression assayed by RT-qPCR.



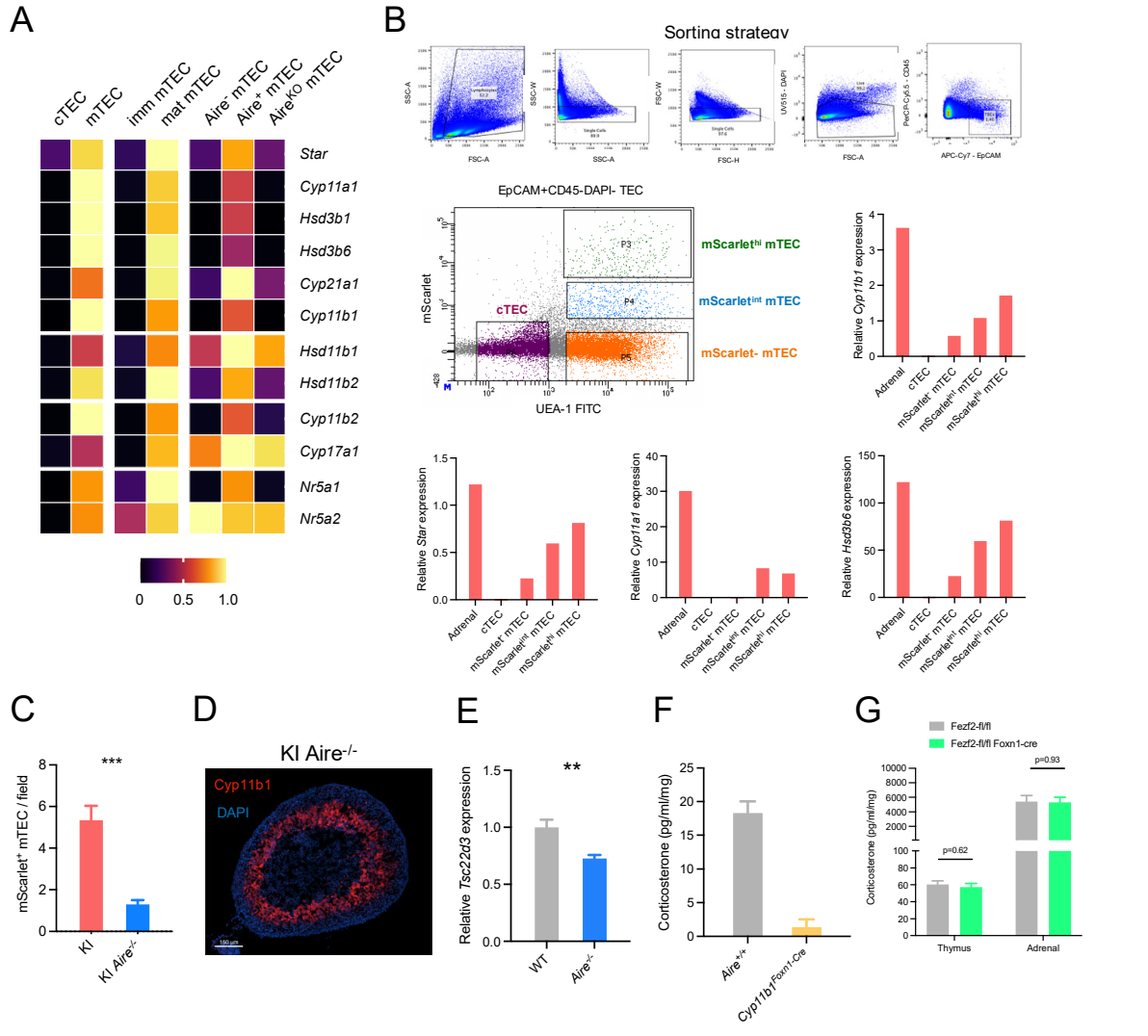
Supplementary Figure 4. Glucocorticoid-synthetic enzymes are expressed in Aire-expressing cells.

(A) UMAPs of single cell RNA-seq data from $Pdpr^{-/-}$ CD104⁺ mTEC^{lo} were analyzed for expression of glucocorticoid-synthetic enzyme genes. Numbered populations in the left panel indicate different cTEC and mTEC cell populations as defined in B. (B) Cell clusters from were analyzed for expression of transcription factors and marker genes associated with specific post-Aire peripheral tissue-mimetic mTEC subsets, as described in (32), and for expression of glucocorticoid-synthetic enzyme genes. mTEC types and their identifying genes are shown in rows, and Seurat-identified cell clusters are grouped in columns. Cell clusters were determined to contain post-Aire peripheral tissue-mimetic cell subsets based on the presence of type-specific transcripts. (C) Pooled thymi from 3 mice were digested, TEC enriched, and total RNA extracted from sorted EpCAM⁺ UEA1⁺ CD45⁻ mScarlet^{hi} mTEC, EpCAM⁺ UEA1⁺ CD45⁻ mScarlet^{lo} mTEC, or EpCAM⁺ UEA1⁻ CD45⁻ cTEC. RT-qPCR was used to quantify relative *Aire* expression normalized to 18S RNA. Expression is shown as the mean of duplicate assay tubes. (D) KI mouse thymi were fixed, sectioned, stained with Aire-A488 and DCLK1-A647, and confocal images were taken at 60 \times oil immersion magnification. Scale bar = 15 μ m. (E) 215 Cyp11b1⁺ mTEC from thymi imaged as in D were categorized by their expression of Aire or DCLK1. (F) KI mouse thymi (n = 3) were digested and cells analyzed by flow cytometry.



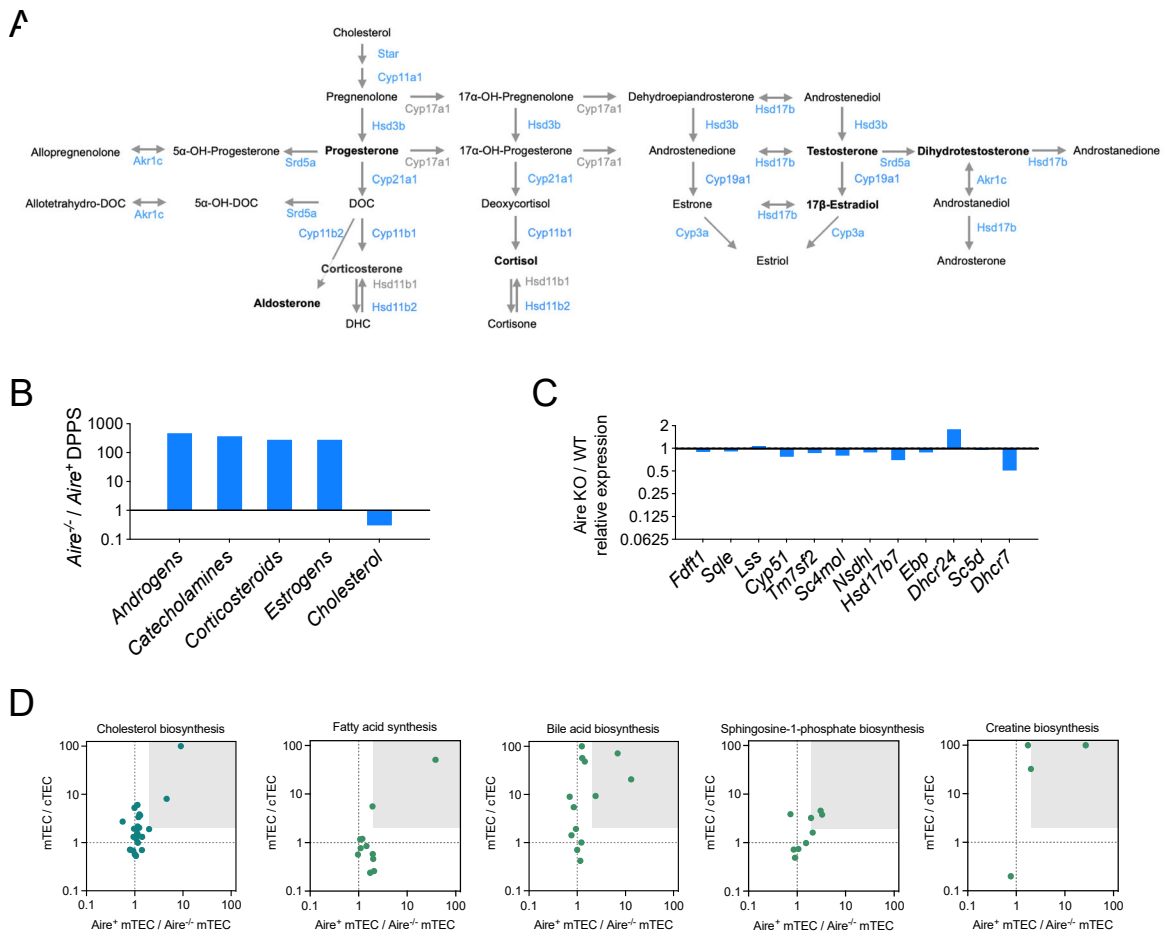
Supplementary Figure 5. *Cyp11b1* is expressed by *Aire*⁺ and post-*Aire* mTEC^{hi} cells.

Thymi from E18.5 (A, B) or 4-7 week-old (C, D) *Cyp11b1*^{mScarlet} knock-in (KI) mice were digested and cells analyzed by flow cytometry (thymocytes: CD45⁺EpCAM⁻MHCII⁻Ly51⁻UEA1⁻; antigen-presenting cells (APC): CD45⁺EpCAM⁻MHCII⁺Ly51⁻UEA1⁻; cTEC: CD45⁻EpCAM⁺Ly51⁻UEA1⁻MHCII⁺; mTEC^{lo}: CD45⁻EpCAM⁺Ly51⁻UEA1⁺MHCII⁺; mTEC^{hi}: CD45⁻EpCAM⁺Ly51⁻UEA1⁺MHCII^{hi}). (A, C) Contour plots show each subset and numbers indicate the percent of cells within the mScarlet⁺ gate. (B, D) Data analyzed as in A and C, pooled from 6 independent experiments (3 at E18.5, 3 at 4-7 wks). Follow-up paired t-tests of KI mouse cell subsets with significance indicated as * p < 0.05, after Holm correction to control family-wise error rate at 0.05.



Supplementary Figure 6. *Aire* is required for mTEC glucocorticoid synthesis.

(A) Gene expression of glucocorticoid biosynthetic enzyme genes in mTEC cell subsets of WT and *Aire*^{-/-} mice. Expression of each gene is presented relative to its maximal expression across analyzed cell types. (B) Pooled thymi from 3 mice were digested, TEC enriched, and total RNA extracted from sorted EpCAM⁺ UEA1⁺ CD45⁻ mScarlet^{hi} mTEC, EpCAM⁺ UEA1⁺ CD45⁻ mScarlet^{int} mTEC, EpCAM⁺ UEA1⁺ CD45⁻ mScarlet⁻ mTEC, EpCAM⁺ UEA1⁻ CD45⁻ cTEC, or whole adrenals. RT-qPCR was used to quantify expression of steroidogenic enzyme genes and normalized to 18S RNA. Expression is shown relative to mScarlet^{int} mTEC cells and shows the mean of duplicate assay tubes. (C) Confocal images of KI and KI *Aire*^{-/-} thymi sections were analyzed by counting the number of mScarlet⁺ cells per field of view (2x2 tiled images with 20 μ m z-stack with 60x objective). Data are presented as mean \pm SEM with N = 18 KI and 20 KI *Aire*^{-/-} fields, and analyzed with an unpaired t-test with significance shown as *** p < 0.001. (D) Adrenals were collected from *Cyp11b1*^{mScarlet} knock-in (KI) *Aire*^{-/-} mice, sectioned, stained with DAPI and anti-mScarlet, and confocal images collected at 20 \times magnification. (E) Total RNA was extracted from whole thymus lobes of WT and *Aire*^{-/-} mice and RT-qPCR used to quantify expression of the Gilz-encoding gene *Tsc22d3* gene. Expression was normalized to 18S RNA and is shown relative to WT expression. Data are pooled from four independent experiments, presented as mean \pm SEM and with N = 17 WT and 9 *Aire*^{-/-} thymi, and analyzed by unpaired t-test with significance shown as ** p < 0.01. (F) Control (*Aire*^{+/+}), *Aire*^{-/-}, or TEC *Cyp11b1* conditional knockout (*Cyp11b1*^{flox/flox} *Foxn1-Cre*) mouse thymi were dissected, minced, and cultured for 72 h in steroid free medium. Supernatants were collected and corticosterone was quantified by ELISA. (G) Control (*Fezf2*^{flox/flox}) or TEC *Fezf2* conditional knockout (*Fezf2*^{flox/flox} *Foxn1-Cre*) mouse thymi and adrenals were dissected, minced, cultured, and assayed as in F.



Supplementary Figure 7. Aire drives mTEC biosynthesis of multiple steroids and other lipid hormones.

(A) Steroidogenic pathway with steroid names in bold and steroidogenic enzyme genes shown in blue (with at least one isoform mTEC-specific and Aire-dependent) or grey (no mTEC-specific and Aire-dependent isoforms). (B) Transcriptomes of Aire⁺ and Aire^{-/-} mTEC were analyzed using the MetaCyc Differential Perturbation Pathway comparison, which uses altered expression of genes in a metabolic pathway to estimate overall disruption of pathway function. Steroid biosynthetic pathways were among the most highly altered pathways in Aire^{-/-} mTEC, while the cholesterol biosynthetic pathways was minimally altered. (C) Gene expression of cholesterol biosynthetic enzyme genes in mTEC cells of WT and Aire^{-/-} mice. Bulk RNA-seq data from Aire^{-/-} mTEC are shown for each gene relative to WT expression of the same gene. (D) mTEC specificity and Aire-dependence of gene expression in biosynthetic pathways of cholesterol, fatty acids, bile acids, sphingosine-1-phosphate, and creatine. Relative expression in Aire⁺ versus Aire^{-/-} mTEC is presented to show Aire-dependent expression, and relative expression in mTEC versus cTEC is presented to show mTEC specificity. The grey box highlights genes with at least a 2-fold expression difference on both axes.

Supplementary Table 1. Key reagent information.

Imaging:

<u>ANTIBODY</u>	<u>SOURCE</u>	<u>REF #</u>
Aire, eBioscience, eFluor 660 (clone 5H12)	Invitrogen	50-5934-82
AIRE mAb, Alexa Fluor 488, eBioscience (clone 5H12)	Invitrogen	53-5934-82
Fluorescein Ulex Europeaeus Agglutinin I (UEA1), FITC	Vector Laboratories	FL-1061
FluoTag-X2 anti-mScarlet-I, Atto 565 (clone 2B12)	NanoTag Biotechnologies	N1302
Hoechst 33342, trihydrochloride, trihydrate	Invitrogen	H3570
Ly-51, Alexa Fluor 647 anti-mouse (clone 6C3)	BioLegend	108312
Cytokeratin 10 Recombinant Rabbit mAb (clone ST05-43)	Invitrogen	MA5-32183
DCLK1 Recombinant Rabbit mAb (clone JA11-03)	Invitrogen	MA5-32657
Goat anti-Rabbit IgG (H+L) Cross-Adsorbed 2 ^o Ab, Alexa Fluor 647	Invitrogen	A-1244

<u>ITEM</u>	<u>SOURCE</u>	<u>REF #</u>
<i>Superfrost plus</i> Microscope Slides Precleaned	Fisherbrand	12-550-15
Coverglass thickness 1 1/2, 22x40mm	Corning	2980-224
Sucrose	Sigma	S0389-500G
O.C.T. Compound	Tissue-Tek	4583
Bovine Albumin Fraction V (BSA)	ICN Biomedicals	810035
Tween 20	Sigma	P2287-500ML
Sodium Chloride	Research Products International	S23020-1000
Glycine Electrophoresis grade	MP Biomedicals	808822
ProLong Glass Antifade Mountant	Invitrogen	P36984

Flow cytometry

<u>ANTIBODY</u>	<u>SOURCE</u>	<u>REF #</u>
Aire mAb, Alexa Fluor 488, eBioscience (clone 5H12)	ThermoFisher	53-5934-82
CD45.2, PerCP-Cy5.5 (clone 104)	BD Biosciences	552950
CD326 (EpcAM), APC/Cyanine 7, anti-mouse, Rat IgG2a (clone G8.8)	BioLegend	118218
CD326 (EpcAM), PE (clone G8.8)	eBioscience	12-5791-82
Cyp11b1, mouse mAb (clone A-11)	Santa Cruz	sc-377401
Cyp11b1, mouse mAb (clone B-11)	Santa Cruz	sc-377248
Cyp11b1, mouse mAb (clone H11)	Santa Cruz	sc-374096
Cyp11b1, goat pAb (V-12)	Santa Cruz	sc-47652
Cyp11b1, rabbit pAb	Bioss	bs-3898R
Cyp11b1, sheep pAb	custom	n/a
Cytokeratin 10 Recombinant Rabbit mAb (clone ST05-43)	Invitrogen	MA5-32183
DCLK1 Recombinant Rabbit mAb (clone JA11-03)	Invitrogen	MA5-32657
Donkey anti-Goat IgG (H+L) Cross-Adsorbed 2 ^o Ab, Alexa Fluor 594	Invitrogen	A-11058

FLAG, mouse mAb (clone M2)	Sigma	F1804
Goat anti-Mouse IgG (H+L) Cross-Adsorbed 2° Ab, Alexa Fluor 594	Invitrogen	A-11032
Goat anti-Rabbit IgG (H+L) Cross-Adsorbed 2° Ab, Alexa Fluor 594	Invitrogen	A-11012
Donkey anti-Sheep IgG (H+L) Cross-Adsorbed 2° Ab, Alexa Fluor 594	Invitrogen	A-11016
Goat anti-Rabbit IgG (H+L) Cross-Adsorbed 2° Ab, Alexa Fluor 647	Invitrogen	A-21244
Live/dead: blue fluorescent reactive dye for UV excitation	Invitrogen	L34962 A
Ly-51, Alexa Fluor 647 anti-mouse (clone 6C3)	BioLegend	108312
Ly-51, Biotin (clone 6C3)	BD Biosciences	553159
MHCII (I-A/I-E), eFluor 450 (clone M5/114.15.2)	eBioscience	48-5321-82
Streptavidin, Alexa Fluor 647 conjugate	InvitrogenTM	S32357
Streptavidin, PE-Cy7	BD Biosciences	557598
Ulex Europaeus Agglutinin I (UEA1), Biotinylated	Vector Laboratories	B-1065-2

Western blot

<u>ANTIBODY</u>	<u>SOURCE</u>	<u>REF #</u>
Beta actin	Sigma	AC-15
Cyp11b1, mouse mAb (clone A-11)	Santa Cruz	sc-377401
Cyp11b1, mouse mAb (clone B-11)	Santa Cruz	sc-377248
Cyp11b1, mouse mAb (clone H11)	Santa Cruz	sc-374096
Cyp11b1, goat pAb (V-12)	Santa Cruz	sc-47652
Cyp11b1, rabbit pAb	Bioss	bs-3898R
Cyp11b1, sheep pAb	Custom	n/a
FLAG, mouse mAb (clone M2)	Sigma	F1804

RT-qPCR

<u>ITEM</u>	<u>SOURCE</u>	<u>REF #</u>
SuperScript IV, First-Strand Synthesis System	Invitrogen	18091050
PowerUp SYBR Green Master Mix	Thermo Fisher Scientific	100029284

PCR assays for Cyp11b1-mScarlet genotyping

<u>ITEM</u>	<u>SOURCE</u>	<u>Sequence 5'-3'</u>
Wild-type/Knock-in Fwd	IDT	CCACGTGGAGACACAAGAGA
Wild-type/Knock-in Rev	IDT	CTCTGACCCCGAATCACAAT
Knock-in Fwd	IDT	CCACGTGGAGACACAAGAGA
Knock-in Rev	IDT	CTGGTCACCTTCAGCTGG

Custom qPCR assays

<u>TARGET</u>	<u>SOURCE</u>	<u>Sequence 5'-3'</u>
18S forward	IDT	AAATCAGTTATGGTTCCTTTGGTC

18S reverse	IDT	GCTCTAGAATTACCACAGTTATCCAA
<i>Aire</i> forward	IDT	CTTGAAACGGAATTCAGAC
<i>Aire</i> reverse	IDT	GAATGCACTTCTGGATCTTC
<i>Cyp11a1</i> forward	IDT	GACCTGGAAGGACCATGCA
<i>Cyp11a1</i> reverse	IDT	TGGGTGTAICTATCAGCTTTATTGA
<i>Cyp11b1</i> forward	IDT	CATTTTCAGGCACAFGTAG
<i>Cyp11b1</i> reverse	IDT	CTCTATGGACTATCCAGGATTC
<i>Hsd3b6</i> forward	IDT	AGACCAGAAACCAGGGAGCAA
<i>Hsd3b6</i> reverse	IDT	TCTCCTCCAACACTGTCACCTT
<i>Tsc22d3</i> forward	IDT	GGTGGCCCTAGACAACAAGA
<i>Tsc22d3</i> reverse	IDT	TCTTCTCAAGCAGCTCACGA

Predesigned qPCR assays

<u>TARGET</u>	<u>SOURCE</u>	<u>REF #</u>
<i>Cyp1a2</i>	IDT	mM.PT.58.18171461
<i>Cyp11b2</i>	IDT	mM.PT.58.10194955
<i>Cyp17a1</i>	IDT	mM.PT.58.10555317
<i>Cyp19a1</i>	IDT	mM.PT.58.30054095
<i>Hsd3b1</i>	IDT	mM.PT.58.43898780
<i>Hsd17b2</i>	IDT	mM.PT.58.17532821
<i>Srd5a2</i>	IDT	mM.PT.58.6711388
<i>Star</i>	IDT	mM.PT.58.33643421
<i>Aire</i>	Sigma	M_Aire_1
<i>Fezf2</i>	Sigma	M_Fezf2_1
<i>Ins2</i>	Sigma	M_Ins2_1
<i>Spt1</i>	Sigma	M_Spt1_1

Data File S1. Cluster 4-specific differentially expressed genes.

List of gene overexpressed in Cluster 4 compared to all other clusters (related to Suppl Fig 4A, B).